Stability of the chevron domain at triple-line reconstructions

Frédéric Lançon,[1,2,*] Tamara Radetic,[2] and Ulrich Dahmen[2]
[1]*Département de recherche fondamentale sur la matière condensée, SP2M/L_Sim, CEA-Grenoble, Cedex 9, 38054 Grenoble, France*
[2]*National Center for Electron Microscopy, Lawrence Berkeley National Laboratory, Berkeley, California 94720, USA*
(Received 10 October 2003; published 13 May 2004)

The line of emergence of a grain boundary at the surface of a face centered cubic crystal may decompose into a nanoscale triangular prism with a chevronlike structure. This behavior has been found in gold, and we address here the generality of this phenomenon. The stability of the chevron structure is studied and discussed for the case of a special tilt grain boundary in copper, nickel, and aluminum. Atomistic simulations predict a chevron decomposition for Cu and Ni, but not for Al. The stability of Al against line decomposition was confirmed by atomic resolution electron microscopy. The distinct behavior of these crystals is related to their stacking fault energies.

DOI: 10.1103/PhysRevB.69.172102 PACS number(s): 61.72.Bb, 61.72.Mm

I. INTRODUCTION

Surface reconstruction is a common mechanism by which atoms at crystal surfaces adapt to a surrounding that is different from that in the bulk. Recently a line reconstruction has been found at the intersection of a grain boundary in gold with the free surface.[1] This new structure corresponds to the dissociation of the junction line into a wire with a nanoscale triangular cross section. The structure and stability of this chevronlike object has been studied by electron microscopy (Fig. 1) and atomistic simulations.

As the atomic arrangement is closely related to hexagonal packing, we believe that the presence of such a reconstruction is not limited to gold, but can be possible in all materials with a low stacking fault energy γ_{sf}.

In this paper, we address the question of its stability in copper, nickel, and aluminum by extending the atomistic model used to study the chevron structure in gold [$\gamma_{sf}=32$ mJ/m^2 for Au (Ref. 2)]. Copper and aluminum have, respectively, low[3] (45 mJ/m^2) and high[4] (166 mJ/m^2) stacking fault energies. Nickel has an intermediate value[4] $\gamma_{sf}=125$ mJ/m^2.

II. INTERATOMIC POTENTIALS

The calculations utilized recent embedded-atom method (EAM) potentials constructed for Cu (Ref. 5), Ni (Ref. 6), and Al.[6] The parameters of these potentials were fitted to experimental values, in particular, the stacking fault energy γ_{sf}, as well as *ab initio* energies, specifically the excess energy δE_{hcp} of the hcp structure over fcc stacking. These potentials were chosen here for their ability to give a good overall agreement with a broad range of properties, but the quantities γ_{sf} and δE_{hcp} are especially important since they control the lateral size of the chevron defect.

III. INCOMMENSURATE INTERFACE GEOMETRY

The dissociation consists of the replacement of the initial grain-boundary termination at the free surface by a domain with triangular cross section, leading to two new grain-boundary segments. Thus the dissociation is unlikely to occur in the case of a low-energy grain boundary. In this section, we describe the geometry and the energy of the $90°\langle 110\rangle$ tilt boundary for which this dissociation was first observed.

An unrelaxed interface, parallel to the $\{y,z\}$ plane, is obtained by joining together two slabs of a fcc crystal. Both slabs have their $[01\bar{1}]$ axes parallel to the z axis, while the y axis is parallel to the [011] direction of the first grain and to the [100] direction of the second grain (see Figs. 1 and 2). This implies that the r_0 interplane periodicity of the first grain is facing the $\sqrt{2}r_0$ interplane periodicity of the second one. To use periodic boundary conditions along the y direction, we need to set integer numbers of planes in two families corresponding to both periods, respectively, n_ℓ and n_s. As $\sqrt{2}$ is an irrational number, this can be done only if a periodic approximant is used instead of the true incommensurate grain boundary. Here we have used the approximation $n_s/n_\ell=41/29\simeq\sqrt{2}-4\times10^{-4}$. Therefore, periodic boundary conditions have been applied to the y (incommensurate) and z (commensurate) directions of the grain boundary, while a free boundary condition has been used in the perpendicular x direction to allow the two grains to shift relative to each other.

The total potential energy E of the N atoms of this configuration, containing one grain boundary and two free surfaces, can be written as $E=NE_{fcc}+S(\gamma_{gb}+\gamma_{(100)}+\gamma_{(011)})$, where S and γ_{gb} are, respectively, the area and the energy of the grain boundary; the other terms are the bulk and surface

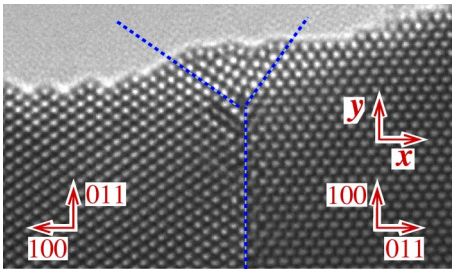

FIG. 1. (Color online) Atomic resolution transmission electron micrograph showing a chevron domain at the intersection of the $90°\langle 110\rangle$ grain boundary with the free surface in gold.

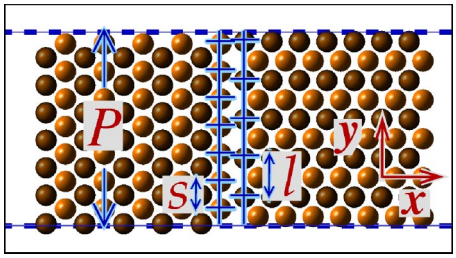

FIG. 2. (Color online) Diagram of a 7:5 approximant of the $90°\langle 110\rangle$ tilt grain boundary corresponding to the approximation $\sqrt{2}\simeq 7/5$. Seven interplane distances s in one grain are facing five distances ℓ in the other grain. The periodicity P of the approximant along the y axis is indicated by the dashed lines. When the model is considered without this boundary condition, it presents two free surfaces perpendicular to the grain boundary and located at $y=0$ and $y=P$, respectively. When larger and larger approximants are used, n_s/n_ℓ and ℓ/s tend to $\sqrt{2}$. A 41:29 approximant has been considered in this paper corresponding to $P\simeq 10$ nm for Cu and with a total width of the model along the x axis equal to 21 nm.

energies of the fcc crystal. The atomic relaxations were calculated by minimizing the energy E with respect to the atomic coordinates. The calculated grain-boundary energies γ_{gb} are 625 mJ/m^2 for Cu, 1060 mJ/m^2 for Ni, and 341 mJ/m^2 for Al.

IV. CHEVRON DOMAIN

Removing the periodic condition along the y direction creates two parallel free surfaces that bound the model perpendicularly to the incommensurate direction of the grain boundary. After another energy minimization, this model without dissociation represents the reference structure for the emergence of the grain boundary at the surface. Subsequently an ''ideal'' model for the chevron structure was obtained by replacing the fcc packing of the atoms in a triangular prism along the z direction by a hexagonal close packing of the same number of atoms (see Fig. 3). In the xy plane, the triangular base has a corner set along the interface

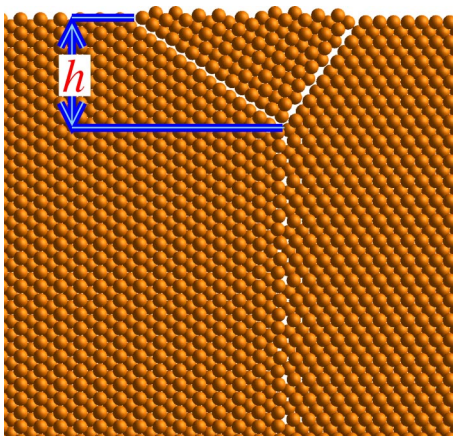

FIG. 3. (Color online) Initial configuration before relaxation toward an ideal chevron structure. The size h of the domain is the height of the triangular fcc region replaced by a hcp packing. Both crystal structures have the same packing fraction.

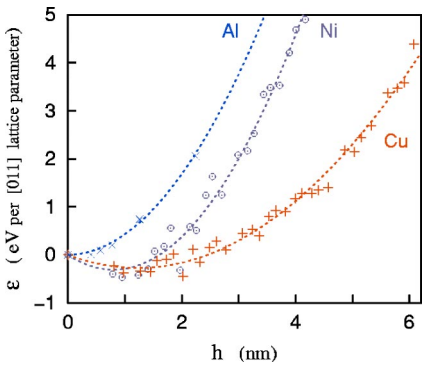

FIG. 4. Variation of the chevron energy per unit length ε with domain size h for aluminum, copper, and nickel. The dashed lines are parabolic fits Ah^2+Bh to these data.

at a distance h from the free surface. One side of the triangle corresponds to the free surface and the other two are parallel to the close-packed planes of the two fcc grains, respectively. Because of the geometry of the interface, the latter two form a right angle. The close-packed planes of the hcp grain are set parallel to the close-packed plane of one grain, leading to stacking faults with respect to the fcc packing. This creates an incommensurate interface along the close-packed plane of the other grain. Therefore, we choose to set this interface along the shortest side of the triangle, i.e., to be the boundary of the second grain (see Fig. 3). Because of the discrete nature of the domain, the size h of the domain can only take discrete values. A sequence of triangles with increasing sizes was constructed by removing the close-packed planes of the two fcc grains one by one.

Because of the crystallographic orientation of the hcp domain, four different configurations have to be considered. They are distinguished by the lattice cell translation with respect to the domain boundaries. For each size h, only the configuration with the lowest energy after the relaxation of the four variants was considered.

The energy ε of the chevron structure as a function of its size h is shown in Fig. 4. In the case of copper and nickel, the minima of $\varepsilon(h)$ are negative and therefore the dissociation of the intersection line leads to a gain in energy. For Cu, the minimum corresponds to the atomic configuration shown in Fig. 5. The optimum size h is about 2 nm, similar to that found in the case of gold.[1] For nickel, the chevron domain size is smaller and about 1 nm. One Ni configuration corresponding to $h=2$ nm, spontaneously created twin interfaces at the triangular domain boundaries and generated a smaller chevron domain ($h\simeq 1$ nm) inside the initial triangle.

In the case of aluminum, the configurations with a small initial hcp domain spontaneously relaxed to the configuration without dissociation. For larger initial hcp domains, most of the stacking faults disappeared during the energy minimization, leaving smaller chevron domains of mainly $4H$ structure and the final energy was always found to be higher. This is consistent with electron microscopy observations that have shown no line dissociation for this grain boundary in aluminum (see Fig. 6). Note that the difference in image quality compared to Fig. 1 is due to differences in the sample and the microscope. Aluminum foils tend to have an amorphous

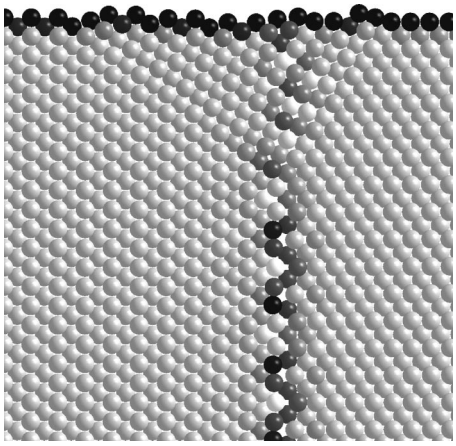

FIG. 5. (Color online) Relaxed Cu chevron structure. Local atomic energy is indicated by shading (white for lowest energies, black for highest energies at the grain boundary; for the higher energies at the surface, the color saturates to black).

oxide surface layer that leads to image noise, especially in very thin samples. In addition, the image in Fig. 6 was recorded on a microscope with athermionic emitter while that in Fig. 1 was taken with a field emission microscope.

V. DISCUSSION

The optimum size of the chevron structure corresponds to the balance between two different energy terms. One term is the excess bulk energy of the chevron defect, proportional to its area in the xy plane. The second contribution is proportional to the length h. This corresponds to the different grain boundary and surface energies, especially the gain of removing the $90°\langle 110\rangle$ interface and the cost of adding two new interfaces. Therefore, the overall shape of the energy $\varepsilon(h)$ of the chevron domain should be of the form Ah^2+Bh.

The fit of this equation is shown in Fig. 4 and corresponds to $A=113\pm 4$ mJ/m^3 and $B=-280\pm 20$ mJ/m^2 in the case of Cu. The energy cost A per volume unit of replacing the fcc lattice by the chevron structure corresponds to an energy per atom equal to 8.4 meV. Although Fig. 5 shows that the initial hcp structure has relaxed to a distorted packing, the A quantity is very close to the hcp excess energy $\delta E_{hcp}=8$ meV (with the same potential; 12 meV by *ab initio* calculation[5]). On the other hand, the energy gain $|B|$ per surface unit of replacing the grain boundary is about half the energy γ_{gb} of this interface (625 mJ/m^2, see Sec. III).

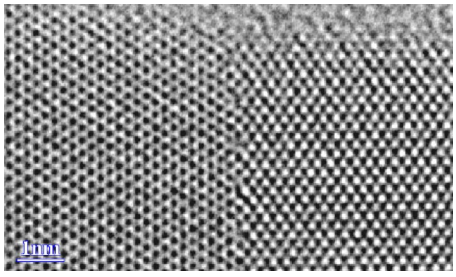

FIG. 6. Transmission electron micrograph of the $90°\langle 110\rangle$ grain boundary in aluminum. No chevron reconstruction occurs at the intersection with the free surface.

In the Al case, the coefficients are $A=231\pm 18$ mJ/m^3 and $B=+10\pm 29$ mJ/m^2. The energy cost A is equivalent to 24 meV per atom, roughly equal to the value 28 meV of δE_{hcp} calculated with the same Al potential. The coefficient B is positive, meaning that there is no energy gain in replacing the grain boundary by the chevron boundaries. Its absolute value is much smaller than in the case of Cu. Taking into account the error bar, we can conclude that this term is negligibly small.

We will now give an expression for the optimal size h as a function of the energy quantities. The area of a chevron domain of size h and the length of its boundaries with the fcc grains are, respectively, $S(h)=3h^2/(2\sqrt{2})$ and $L(h)=\sqrt{3}(1+1/\sqrt{2})h$. Thus the energy ε of introducing a chevron of size h can be approximated as $\varepsilon(h)=[\gamma_{cb}L(h)-\gamma_{gb}h]+\delta E_{hcp}S(h)/V_0$, where γ_{cb} is the mean grain-boundary energy of the chevron domain and V_0 is the atomic volume. The energy $\varepsilon(h)$ has a minimum at $h=V_0[\sqrt{2}\gamma_{gb}-(1+\sqrt{2})\sqrt{3}\gamma_{cb}]/(3\delta E_{hcp})$. The energy of the interfaces bounding the domain is closely related to the stacking fault energy and therefore we make the approximation $\gamma_{cb}=\gamma_{sf}$. The excess energy δE_{hcp} can also be related to the stacking fault energy in a first approximation. The stacking sequences of the close-packed structures can be described by an Ising model[7,8] where the translations between successive planes are represented by spins and the hcp crystal is deduced from the fcc crystal by introducing stacking faults every two close-packed planes. Using a first neighbor interaction approximation in this Ising-model analogy, leads to $\delta E_{hcp}=\sqrt{3}r_0^2\gamma_{sf}/4$. The accuracy of this relation can be checked here, since both quantities can be computed with the interatomic potentials used in this paper. Using γ_{sf} as input, it gives δE_{hcp} with errors equal to 0.3, 4, and 16 % for Cu, Ni, and Al, respectively. With these approximations, and approximating also $\sqrt{3}+\sqrt{3/2}\simeq 2.96$ to 3, the optimal chevron size is given by

$$h=h_0[(\gamma_{gb}/\gamma_{sf})-3] \tag{1}$$

where

$$h_0=(2/3)^{3/2}a,$$

and where a is the fcc lattice parameter. The triple-line reconstructs into a chevron domain when

$$\gamma_{gb}/\gamma_{sf}>3. \tag{2}$$

Table I shows that relation (1) gives values close to the minimum location of the Cu and Ni curves in Fig. 4 and in agreement with the chevron sizes found by electron microscopy on gold. In the case of aluminum, the above relation shows that no dissociation should occur. This is in agreement with the Al curve in Fig. 4 and the experimental results. Note that because of the nature and the construction of the EAM potentials, there are small discrepancies between the experimental values of γ_{sf} and the values calculated with these potentials. However, when used with the relation (2), both values lead to the same conclusion.

TABLE I. Grain boundary and stacking fault energies γ_{gb} and γ_{sf}. These quantities have been calculated with the interatomic potentials used in this paper, unless otherwise stated. The chevron size h has been estimated using Eq. (1) (where no means not stable).

	γ_{gb} (mJ/m^2)	γ_{sf} (mJ/m^2)	γ_{gb}/γ_{sf}	h (nm)
Cu	625.0	44.4	14.1	2.2
Au	335.0[a]	32.0[b]	10.5	1.7
Ni	1060.0	125.0	8.5	1.0
Al	341.0	146.0	2.3	no

[a]From Ref. 9.
[b]From Ref. 2.

Because the $90°\langle 110\rangle$ grain boundary is nonperiodic, the core energy of the intersection of the three interfaces is going to vary with its position h. This also implies a similar behavior for the two corners at the free surface. The core energies of the corners lead to the distribution of the ε values around the parabolic curves. Because the absolute position of the surface with respect to the incommensurate interface structure depends on initial macroscopic conditions, the optimum size and structure of chevron domains are also going to be distributed.

VI. CONCLUSION

The emergence of the $90°\langle 110\rangle$ tilt grain boundary at the surface perpendicular to its incommensurate direction has been observed by atomic resolution electron microscopy in gold and in aluminum. The intersection line reconstructs into a prismatic chevron domain in gold, while no reconstruction occurs in aluminum.

Using atomistic simulations, these results have been confirmed and extended to copper and nickel. The stacking fault energy plays a critical role in the energy balance that controls the reconstruction. A simplified model predicts that the dissociation occurs only when $\gamma_{gb}/\gamma_{sf} > 3$, and the defect size is approximately $h = (2/3)^{3/2} a[(\gamma_{gb}/\gamma_{sf}) - 3]$.

ACKNOWLEDGMENTS

This work was supported by the Director, Office of Science, Office of Basic Energy Sciences, Division of Materials Sciences and Engineering, of the U.S. Department of Energy under Contract No. DE-AC03-76SF00098. F.L. acknowledges the hospitality of NCEM during a research leave at Berkeley Lab.

*Email address: FLancon@cea.fr

[1] T. Radetic, F. Lançon, and U. Dahmen, Phys. Rev. Lett. **89**, 085502 (2002).
[2] J.P. Hirth and J. Lothe, *Theory of Dislocations*, 2nd ed. (Wiley, New York, 1982).
[3] C.B. Carter and I.L.F. Ray, Philos. Mag. **35**, 189 (1977).
[4] L.E. Murr, *Interfacial Phenomena in Metals and Alloys* (Addison-Wesley, Reading, MA, 1975).
[5] Y. Mishin, M.J. Mehl, D.A. Papaconstantopoulos, A.F. Voter, and J.D. Kress, Phys. Rev. B **63**, 224106 (2001).
[6] Y. Mishin, D. Farkas, M.J. Mehl, and D.A. Papaconstantopoulos, Phys. Rev. B **59**, 3393 (1999).
[7] F. Ernst, M.W. Finnis, D. Hofmann, T. Muschik, U. Schönberger, U. Wolf, and M. Methfessel, Phys. Rev. Lett. **69**, 620 (1992).
[8] P.J.H. Denteneer and J.M. Soler, Solid State Commun. **78**, 857 (1991).
[9] F. Lançon, J.-M. Pénisson, and U. Dahmen, Europhys. Lett. **49**, 603 (2000).